



eTAG: An Energy-Neutral Ear Tag for Real-Time Body Temperature Monitoring of Dairy Cattle

Hien Vu, Hanwook Chung, Christopher Y. Choi, and Younghyun Kim

University of Wisconsin–Madison

Madison, Wisconsin, USA

{hien.vu,hchung45,cchoi22,younghyun.kim}@wisc.edu

ABSTRACT

Heat stress, caused by a warming climate and the increasingly high milk-producing dairy cattle, is one of the major threats to the well-being of dairy cattle as well as the economic, environmental, and social sustainability of dairy farming around the world. Timely identification of cows under heat stress is crucial to improving animal welfare, preventing milk production losses, and preserving water and energy for cooling.

This paper presents a smart ear tag, named eTAG, and an associated system that can read a passive microchip temperature sensor subcutaneously injected into the animal with minimal discomfort. It features a lightweight design using a single coil shared for microchip scanning and wireless charging. eTAG is autonomously recharged by a wireless charger over the head during daily milking sessions, enabling perpetual operation without battery replacement after deployment. The real-world performance of the proposed system was examined intensively in a three-week deployment on seven lactating Holstein cows. We demonstrate that eTAG can reliably collect accurate body temperature in real time while maintaining a positive energy flow. The deployment of eTAG will enable the timely detection of heat stress and facilitate precision control of barn cooling systems.

CCS CONCEPTS

• **Applied computing** → **Agriculture**; • **Hardware** → **Wireless devices**.

KEYWORDS

Precision livestock farming, real-time health monitoring, wearable device, energy harvesting

Permission to make digital or hard copies of all or part of this work for personal or classroom use is granted without fee provided that copies are not made or distributed for profit or commercial advantage and that copies bear this notice and the full citation on the first page. Copyrights for components of this work owned by others than the author(s) must be honored. Abstracting with credit is permitted. To copy otherwise, to republish, to post on servers or to redistribute to lists, requires prior specific permission and/or a fee. Request permissions from permissions@acm.org.
ACM MobiCom '23, October 2–6, 2023, Madrid, Spain
© 2023 Copyright held by the owner/author(s). Publication rights licensed to ACM.

ACM ISBN 978-1-4503-9990-6/23/10...\$15.00

<https://doi.org/10.1145/3570361.3613262>

ACM Reference Format:

Hien Vu, Hanwook Chung, Christopher Y. Choi, and Younghyun Kim. 2023. eTAG: An Energy-Neutral Ear Tag for Real-Time Body Temperature Monitoring of Dairy Cattle. In *The 29th Annual International Conference on Mobile Computing and Networking (ACM MobiCom '23)*, October 2–6, 2023, Madrid, Spain. ACM, New York, NY, USA, 15 pages. <https://doi.org/10.1145/3570361.3613262>

1 INTRODUCTION

The dairy industry worldwide is facing the pressures of continued economic viability and acceptability to society at large, and heat stress is one of the most daunting challenges toward both goals. Excessive heat can increase the incidence of illnesses and fatalities [45, 48] that threaten animal well-being [44], while it can also cause reductions in reproductive efficiency [14] and milk yield [50]. A recent study estimated that heat stress could cost the global dairy industry up to 9.14 billion USD annually by the end of this century [47], and it will only become worse with the accelerating global climate change [6].

As dairy herds become larger and more cows are housed in confined facilities, the risk of heat stress is only increasing. In the U.S., for instance, larger barns (with more than 500 cows) are increasingly responsible for more of the total milk production. However, ventilation systems in these dairy barns often rely only on environmental-based heat stress indicators such as ambient air temperature and humidity as operational thresholds [3, 37]. Because each dairy cow experiences heat stress differently due to different metabolic heat generation [20, 27, 49], and these ambient parameters alone are not sufficient to reflect the internal state of the cows as they are just a few among many factors that contribute to heat stress [37], such systems could either underperform or overperform, failing to address heat stress problem while also consuming unnecessarily large amounts of electricity and water [19]. Thus, early and accurate detection of heat stress of individual cows is essential for improving animal welfare, minimizing production losses, and preserving resources.

Dairy cows experiencing heat stress exhibit several physiological changes, including increased core body temperature (CBT), respiration rate, and heart rate, as well as reduced physical activities, milk yield, and feed intake [21]. Among these parameters, CBT is considered the most valuable for assessing heat stress and has been extensively studied [21, 32].

Table 1: Comparison of continuous body temperature monitoring techniques

Measurement location	Administration	Device and size	Real-time	Accuracy ^(a)	Power source
Vagina or rectum [46]	Insertion	9.2×2.0-cm data logger ^(b)	No	Reference	Battery
Reticulum [34]	Ingestion	11.0×2.5-cm bolus ^(b)	Yes	Medium	Battery
Inside the body [2, 12, 30, 39]	Implantation	Wireless telemetries (various sizes)	Yes	High ($R^2 = 0.87$)	Battery
Ear base [9]	Neck-mounted ^(d)	21.0×7.0-cm halter device ^(b)	Yes	High ($R^2 = 0.73$)	Battery
Rectal and abdominal skin regions [40]	N/A	3.0×3.0-cm sensor probe ^(e)	Yes	High ($R^2 = 0.73$)	N/A
Eye/ear/horn [7, 24, 28, 38]	None	Infrared camera & other sensors ^(c)	Yes	High ($R^2 = 0.83$)	N/A
(Human) forehead [26]	Head-mounted	1.5×3.5-cm sensor probe ^(c, e)	N/A	Medium ^(f)	N/A
(Human) ear drum [42]	In-the-ear	Slightly bigger than the ear	Yes	N/A ^(f)	Battery
Ear base (this work)	On-the-ear ^(d)	1.5×11.0-cm ear tag ^(b)	Yes	High	Wireless charging

^(a) Representing how well the measurement reflects CBT without being affected by environmental and behavioral disturbances.

^(b) Length or thickness, and diameter of the cylindrical or disc-shaped device. ^(c) Installed at a fixed distance from the cow.

^(d) Location of the wearable scanner that scans a 12×2-mm injected microchip temperature sensor.

^(e) Size of the sensor probe only. Additional device is required to read the sensor. ^(f) Not applicable to cows.

However, measuring the CBT of dairy cows is not trivial. Various methods have been proposed, such as rectal temperature loggers [5], ingestible biosensors [34], implantable wireless temperature sensors [30], wearable temperature loggers [9], and infrared cameras [38]. While these methods have shown feasibility in specific cases, they are often labor-intensive, inaccurate, non-real-time, overly invasive, and/or unsuitable for long-term monitoring. As a result, farmers still predominantly rely on indirect environmental-based indicators of heat stress that lag behind and do not necessarily represent a cow's level of thermal discomfort.

In this paper, we introduce a continuous body temperature measurement system for dairy cattle that is perpetual, accurate, real-time, and minimally invasive. These objectives are achieved through the use of an energy-harvesting ear-mounted wearable device named eTAG that can continuously read a microchip temperature sensor. The microchip sensor is subcutaneously injected using a syringe without surgical operation (thus minimally invasive) and can accurately measure body temperature without being affected by external factors. eTAG is autonomously recharged with sufficient energy for perpetual operation through a wireless charger during daily milking sessions. It features a novel coil-sharing design that reads the sensor and receives wireless power using the same coil, reducing the size and weight that enables the device to be integrated into the form of an ear tag. This design offers significant advantages for adoption in the field, as all dairy cows in commercial dairy farms are already accustomed to ear tags for cow identification.

In summary, the main contributions of this work are as follows:

- (1) We design and implement a minimally invasive real-time body temperature monitoring system for dairy cattle using an energy-neutral ear tag named eTAG that can measure and report the body temperature of

cows. The device can operate perpetually by receiving wireless power during regular milking sessions.

- (2) We present a fully automated wireless charging system that efficiently and safely charges eTAG mounted on the moving head. The design of the wireless charger is fully compatible and scalable with the existing infrastructure of modern dairy barns.
- (3) We provide deployment and evaluation results of eTAG on seven lactating Holstein cows and the proposed wireless charger in a three-week experiment, totaling 1966 hours of run-time and 17 charging sessions at an operational dairy barn.

2 RELATED WORK

Many works have been proposed on continuous body temperature monitoring of dairy cattle, as it is one of the most important factors for understanding their health status, including heat stress level. Table 1 compares various techniques.

The most common practice is recording temperature using a temperature logger inserted in the vagina or rectum [46], and is usually used to provide the reference CBT [21, 32]. However, the insertion of the device is invasive to the cow, and the device needs to be retrieved for data extraction, and hence it cannot be used for real-time monitoring.

To enable real-time temperature monitoring, an ingestible biosensor can be used to measure the reticulum temperature [34]. While this is less invasive as the sensor is orally administered, the measurement is susceptible to disturbances from feeding and drinking activities. Moreover, these devices can only run for several months, whereas the average productive lifespan of dairy cows is around four years [15], making this method less suitable for long-term monitoring.

There exist surgically implantable wireless temperature sensors such as [30] with a strong correlation with the CBT ($R^2 = 0.83$), as well as some commercial wireless telemetries

such as Stellar Telemetry [39] (TSE Systems, Chesterfield, MO, USA), PhysioTel M-series [2] (Harvard Bioscience Inc., St. Paul, MN, USA), and CubiSens TS110 [12] (CubeWorks, MI, USA). However, surgical implantation, as opposed to simple injection, is prohibitively costly and invasive.

Wearable devices can be a low-cost solution to real-time body temperature monitoring. A neck-mounted device was proposed in [9] that scans a microchip temperature sensor, which is subcutaneously injected at the cow's ear base. The device is attached to a neck strap to continuously scan the microchip sensor in real time. While this method provides a minimally invasive way to accurately measure body temperature ($R^2 = 0.73$), the device has a prohibitively short lifespan and impractical size. It can run for only a few weeks even with a large battery, which increases deployment costs and causes discomfort to the animal.

In [40], the body temperature of cows was measured from the surface temperatures across the rectal and abdominal regions using infrared photodiode thermometers. Although the correlation between the measured temperature and the rectal temperature was high ($R^2 = 0.73$), the measurement devices are required to be mounted at unusual parts of the cow, which significantly degrades the well-being of the animal.

The use of stationary infrared cameras to estimate body temperature was also investigated [7, 24, 28]. Various measurement points were chosen, such as the eyeball or the posterior ear region, and moderate correlations between the measured and rectal temperatures were achieved (the highest $R^2 = 0.50$). However, the measurement is prone to effects from animal parameters such as hair coat and metabolism, while it can also be significantly influenced by the distance of measurement [28] and the oscillations of environmental conditions [24]. The correlation was further improved by combining thermal images with environmental parameters (ambient temperature, humidity, and illuminance) and moving distance to achieve $R^2 = 0.83$ [38]. Nonetheless, it is highly dependent on the visibility of the measurement point, which is influenced by animal posture and movement.

Some techniques developed for human subjects can also be considered for comparison. A combination of a temperature sensor and a heat flux sensor was used to measure the rate of heat loss on the skin surface to estimate the rectal temperature ($R^2 = 0.64$) [26]. However, this approach is not applicable to dairy cows as their hair, sprayed water, and heavy dirt will prevent the sensor from staying on the skin. Another study proposed to use a wearable thermopile infrared (IR) sensor to measure the temperature of the tympanic membrane in real time for estimating body temperature [42]. Nonetheless, this is also not a suitable form of sensor for long-term application to dairy cows in the field as their inner ears are sensitive to foreign objects.

In summary, despite its importance, there has not been a solution for reliable, long-lasting, real-time, and minimally invasive body temperature measurement.

3 SYSTEM DESIGN

As discussed in Section 2, previous continuous body temperature monitoring techniques fall short in one or more ways. In this section, based on the previously examined works, we first discuss the requirements of a continuous body temperature monitoring system for dairy cattle. We discuss various sensing approaches for measuring CBT and design choices. Next, we present an overview of the proposed system that is judiciously designed and optimized to meet the requirements. We also provide detailed analyses on the specifications of the system for practical deployment.

3.1 System Requirements

A continuous body temperature monitoring system for dairy cows must meet the following requirements.

Minimal invasiveness. To ensure the welfare of the cows, the application of a device should be minimally invasive, and it should not cause any significant discomfort to the animal during deployment and usage. Therefore, it must be small and lightweight, so it can be easily ingested, injected, or worn. If any wearable device is involved, it must be in a form familiar to cows, such as an ear tag or a neck collar. Minimal invasiveness is also crucial for reducing labor costs for applying and maintaining a large number of devices.

High measurement accuracy. Ideally, a device should be capable of directly measuring the CBT, such as the vaginal or rectal temperature. Alternatively, a temperature that accurately reflects CBT, such as subcutaneous temperature, can be measured. Skin temperature and rumen temperature can be interfered by external factors (e.g., water) or behavioral factors (e.g., water intake).

Real time. For timely detection and mitigation of heat stress, real-time measurement is necessary, rather than logging for later retrieval. This requires wireless communication capability, with a transmission range of at least tens of meters to effectively cover the modern free-stall barn where cows can move freely within their pens. As a substantial change in CBT can occur in a short period, a shorter sampling interval (order of minutes) will be required.

Long lifespan. To minimize maintenance costs, the system should outlast the cows' lifespan, which is typically from three to four years [15]. It should withstand the harsh environment of the barn with a lot of water, dust, and movement of the heavy animals. Once applied, the system should be operational without maintenance, such as battery replacement or recharge, throughout its lifetime, i.e., energy-neutral.

3.2 Design Space Exploration

We explore design space to derive a practical real-time temperature monitoring system for dairy cattle that meets the requirements outlined in Section 3.1.

Scanning the microchip temperature sensor remotely. Using an injectable microchip temperature sensor is the basis

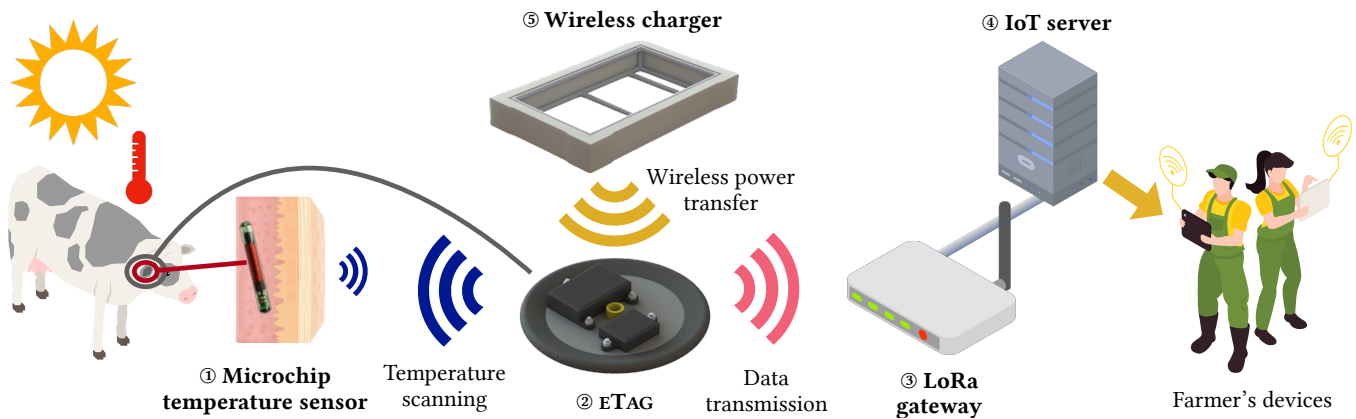


Figure 1: Overview of the proposed real-time body temperature monitoring system for dairy cattle using eTAG

of the high-accuracy CBT measurement we aim at. Ideally, long-range one-hop scanning of microchip temperature sensors would be preferable for a simple and energy-efficient design. Some passive Ultra-High Frequency (UHF) RFID temperature sensors can be scanned at a long distance of up to 4 m [51]. However, due to the strong attenuation of UHF signals through body tissues [17], UHF temperature sensors are not suitable for injectable microchips. As a result, the Low-Frequency (LF) band is used for injectable microchips as in the ISO 11784/5 standards [33] despite its relatively short scanning range of about 10 cm [8]. Therefore, a two-hop topology is needed, where an intermediate wearable device reads the temperature sensor using the short-range LF band, which is then forwarded to a stationary receiver using a long-range wireless link. For high energy efficiency, long range, low data rate, and high scalability, LoRa is an ideal choice for data forwarding. The use of LoRa for barn monitoring has been widely studied and shown to be practical [4].

Powering the intermediate wearable device perpetually. Scanning a microchip sensor consumes more than 700 mW of power and 250 mJ of energy on average. With a 5-minute scanning interval, daily energy consumption would be more than 70 J (about 20 mWh). Rechargeable batteries with energy harvesting would be the only viable option to supply this energy, as non-rechargeable batteries cannot last multiple years of the cow's lifespan. Energy harvesting sources such as solar, RF, acoustic, and body heat have power densities of less than $10 \mu\text{W}/\text{cm}^2$ in indoor environments, rendering them insufficient to power the device throughout the day [1]. A feasible approach is wireless power transfer (WPT) which can provide a significant amount of electrical energy. There are several common WPT techniques such as inductive coupling [11], resonant inductive coupling [52], and magnetic resonant coupling [35]. Among these, resonant inductive coupling offers reasonable power transfer performance and transfer range while imposing minimal hardware overhead, making it an optimal choice.

3.3 Overview of the Proposed Design

The main goal of this work is to develop a minimally invasive method for continuously measuring the body temperature of dairy cattle in real time. This is accomplished by using (i) a lightweight wearable ear tag that can scan a microchip temperature sensor injected in the ear base and wirelessly send the data to a server, and (ii) a wireless charging system that can autonomously recharge the ear tag. Called eTAG, the proposed system meets all the requirements discussed in Section 3.1: (i) The injectable microchip temperature sensor and eTAG are minimally invasive to the cows, (ii) the sensor measures the subcutaneous temperature that is highly correlated with the CBT, (iii) data is collected wirelessly in real time, and (iv) the autonomous wireless charging enables perpetual operation.

A high-level overview of the proposed system is depicted in Figure 1. A bio-compatible microchip temperature sensor (1) is injected subcutaneously through a quick and painless injection procedure. The microchip sensor is a passive RFID device powered by an external scanner, and so once injected, it remains operational permanently without replacement. We use a commercial off-the-shelf microchip temperature sensor, LifeChip Bio-Thermo ($\pm 0.1^\circ\text{C}$ accuracy, 2×12 mm, Destron Fearing Fort Worth, Texas, USA), but any passive RFID microchip temperature sensor that is compliant with ISO 11784/5 [33] can be used. The eTAG (2) periodically interrogates the microchip sensor to obtain the current temperature and sends the reading to a LoRa gateway (3). The gateway forwards the data to an IoT server (4) where they are collected, analyzed, and visualized in real time.

The subcutaneous microchip sensor is able to accurately measure body temperature [9], but the high accuracy comes with the cost of high power consumption for scanning the sensor through RFID backscattering. To power the scanner using a small battery that can hold only a few days' worth of energy, we add wireless charging capability to eTAG. A wireless charger (5) is installed over the head at the milking

parlor. Cows are milked at least once per day, typically every 12 hours. They are milked automatically in batches that take only about 10–15 minutes per batch. As the cows routinely visit the milking parlor, charging eTAG during milking allows one charger to charge many tags each day.

The lightweight design of eTAG is realized by a novel RF circuit design and wireless charging. To enable perpetual operation with a minimal battery and short charging duration, we implement various schemes to maximize the power transfer efficiency and minimize the power consumption of eTAG. Additionally, we incorporate safeguards to ensure the safety of the cows during wireless charging. The details of eTAG and the wireless charger design are elaborated in Sections 4 and 5, respectively.

3.4 Energy Neutrality Analysis

We further discuss energy neutrality, which is the key property to meet for practical deployment. We present an energy model to determine various important design parameters of the system to ensure the energy neutrality of eTAG.

In modern milking parlors, the duration of milking one cow, that is equivalent to the duration of charging, T_{charge} , which is relatively short as farmers try to milk as many cows as possible with as few milking machines as possible. This limits the amount of energy eTAG can receive in one charging session, E_{charge} . To minimize the required charging frequency, eTAG should be able to store all received wireless energy without overflow. Therefore, the ideal battery capacity would be:

$$E_{bat} = E_{charge} = P_{charge} \cdot T_{charge}. \quad (1)$$

The energy consumption of eTAG during one wake-up interval, T_{wake_intv} , consists of the energy consumption in sleep mode, E_{sleep} , and during wake-up, E_{wake} . Here, E_{sleep} is a function of T_{wake_intv} such that $E_{sleep} = P_{sleep} \cdot T_{wake_intv}$ while E_{wake} is dependent on the success rate of scanning the microchip sensor, η_{scan} ($0\% \leq \eta_{scan} \leq 100\%$). The number of wake-ups between two consecutive charging sessions can be defined as:

$$n_{wake} = \frac{E_{bat}}{E_{wake} + P_{sleep} \cdot T_{wake_intv}}. \quad (2)$$

From (1) and (2), the total runtime of the device from a single charge is:

$$T_{run} = n_{wake} \cdot T_{wake_intv} = \frac{P_{charge} \cdot T_{charge} \cdot T_{wake_intv}}{E_{wake} + P_{sleep} \cdot T_{wake_intv}}. \quad (3)$$

For example, assuming eTAG scans the microchip sensor every 5 minutes, $E_{wake} = 300$ mJ, and E_{sleep} is negligible, if the charger provides 1 W to eTAG in 10 minutes, the runtime in one charge will be about 7 days. In this case, a 3.7-V 45-mAh battery would be needed to store the charging energy.

In a dairy facility with N_{cows} cows and $N_{chargers}$ chargers, the number of milking batches $N_{batches}$ is the number of

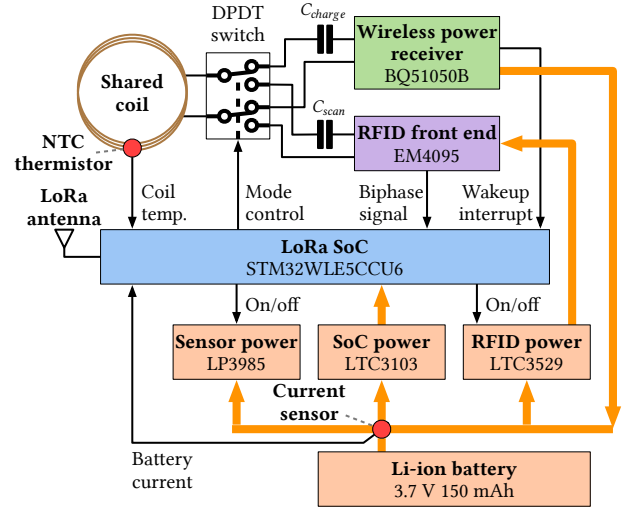


Figure 2: Block diagram of eTAG showing control signals and power supplies

devices each charger can charge per day. The duration to charge all eTAGs at least once, or the interval that the charger can recharge the tags is:

$$T_{charge_intv} = \frac{N_{cows}}{N_{chargers} \cdot N_{batches}}. \quad (4)$$

To ensure the energy neutrality of eTAG, the tag should be recharged before it runs out of battery such that $T_{charge_intv} \leq T_{run}$. The ideal condition is when T_{charge_intv} is maximized:

$$T_{charge_intv} = T_{run}. \quad (5)$$

Combining (4) and (3) into (5), we obtain:

$$N_{chargers} = \frac{N_{cows}(E_{wake} + P_{sleep} \cdot T_{wake_intv})}{N_{batches} \cdot P_{charge} \cdot T_{charge} \cdot T_{wake_intv}}, \quad (6)$$

As an example, for a dairy facility with 100 cows, each cow with one eTAG, if there are six milking batches per day at the milking parlor, according to (6), only three chargers are needed to ensure the perpetual operation of all tags.

4 ETAG: ENERGY-HARVESTING TEMPERATURE SCANNING EAR TAG

This section introduces the design of eTAG focusing on small, lightweight implementation in the form of an ear tag. We first present a novel circuit design for scanning the microchip sensor and charging wirelessly using a shared coil. Next, we describe hardware and software implementation for low-power operation.

4.1 Functional Blocks of eTAG

The main blocks of eTAG with interface connections and power supplies are depicted in Figure 2. eTAG has three modes of operation: scanning mode (reading temperature from the microchip sensor), charging mode (receiving power

to recharge the battery), and sleep mode (waiting for the next scan and not receiving power).

The LoRa system-on-chip (SoC) is the main processor of eTAG for sensing, computation, and communication. In scanning mode, the RFID front-end circuit energizes the microchip sensor and receives the temperature data through backscattering. The LoRa SoC decodes the RFID front-end signal which contains the current temperature, and transmits the data to the LoRa gateway, while also controlling other functional blocks. When wireless power is available at the coil, the wireless power receiver rectifies and converts the received power to charge the Li-ion battery. It also triggers a wake-up interrupt to switch the LoRa SoC to the charging mode where it measures various device status parameters to send to the wireless charger, such as the coil temperature, battery charging current, and battery voltage. A single coil is shared by the RFID front-end and the wireless power receiver, as described in detail in Section 4.2. A switching circuit is used to connect the shared coil to the RFID front-end in scanning mode or to the wireless power receiver in charging mode. Three voltage regulators are used to power various components.

Various techniques are employed to minimize the power consumption of eTAG. First, we implement low-power RFID decoding directly on the LoRa SoC. Commercial RFID scanners are usually designed for various tasks and to work with different RFID standards. While they offer compatibility with diverse types of RFID tags and microchips, this leads to longer scanning and decoding times. Because the microchip sensor used in this system is a specific type of RFID microchip that is compliant with ISO 11784/5, using a universal RFID scanning circuit would unnecessarily waste power. Therefore, the demodulated biphasic signal from the RFID front-end is fed into the LoRa SoC and is decoded using the FDX-B protocol specified in ISO 11784/5. As a result, we achieve a significant reduction in the scanning time from 1.5 s (using a typical commercial device) to only 0.1 s when the coil and the microchip sensor are in good alignment. Since the microchip sensor scanning is the most power-consuming task, reducing the scan time by 15× significantly extends the runtime of eTAG. We put the LoRa SoC into power-saving sleep mode between scanings to minimize its idle power consumption. Power consumption is further minimized by independent power gating for various peripherals, such as the RFID front-end and the sensing unit.

eTAG reports temperature values to the IoT server after each scanning using LoRa. During charging, eTAG also utilizes LoRa to pass the device status to the wireless charger to enable closed-loop control that adjusts the level of wireless power at the primary coil based on the amount of power it receives. The control of wireless charging is discussed in Section 5.

Although cyclic redundancy check (CRC) is embedded in the RFID packets, the CRC in the FDX-B protocol only

protects the ID field, but not the temperature readings in the extra data field. As a result, an incorrect temperature value can occasionally be received. Temperature values that fall outside the biologically relevant range of 35–42 °C are ignored.

4.2 Shared Coil for Microchip Sensor Scanning and Wireless Charging

As described in Section 3.3, eTAG is essentially a microchip sensor scanner that is wirelessly rechargeable. However, designing such a device as an ear tag poses many challenges. Due to the stringent weight and size constraints, having two dedicated coils for microchip sensor scanning and wireless charging would not be a desirable design as each copper coil will add to the mass of the device. In addition, with two coils in the same ear tag, their close proximity will create a mutual coupling effect such that the electrical properties of each single coil will be altered significantly from their original parameters. For instance, when scanning the microchip sensor, the scanner coil would create a resonant electromagnetic field that induces a current in the charging coil, thereby reducing the amount of useful energy the microchip sensor can receive. The mutual coupling effect would also change the resonant frequency of the resonant circuit for scanning that greatly reduces the reading distance of the scanner. Similarly, when the charging coil is used to receive power during charging, the resonant frequency of the charging circuit will be shifted, resulting in poor power transfer efficiency.

We address this problem by sharing a single coil for both microchip sensor scanning and wireless charging with judiciously designed switching and matching circuits. The scanning circuit and the charging circuit employ the same mechanism of series-series inductive resonant coupling, but they require opposite properties because it acts as a primary coil for scanning but as a secondary coil for charging. For scanning, the coil needs to be tuned to maximize the scanning range with low power consumption. For this, a high-inductance high-resistance coil is preferred to generate a sufficient peak-to-peak resonant voltage at a low current. On the other hand, for wireless charging, a high-inductance low-resistance coil is preferred to minimize power loss due to ohmic resistance in the coil. Otherwise, the received power will be lost as heat that increases the coil temperature during charging, which could damage the device or cause discomfort to the cow. Given the opposite design goals, the wire gauge and the number of turns of the coil should be carefully determined so that both microchip scanning performance and wireless charging performance are balanced, i.e., the energy consumed for scanning does not exceed the energy received during short milking sessions. We used Keysight PathWave ADS and Ansys Electromagnetics to determine the optimal coil design. The specific coil properties that achieve these goals are described in Section 4.3.

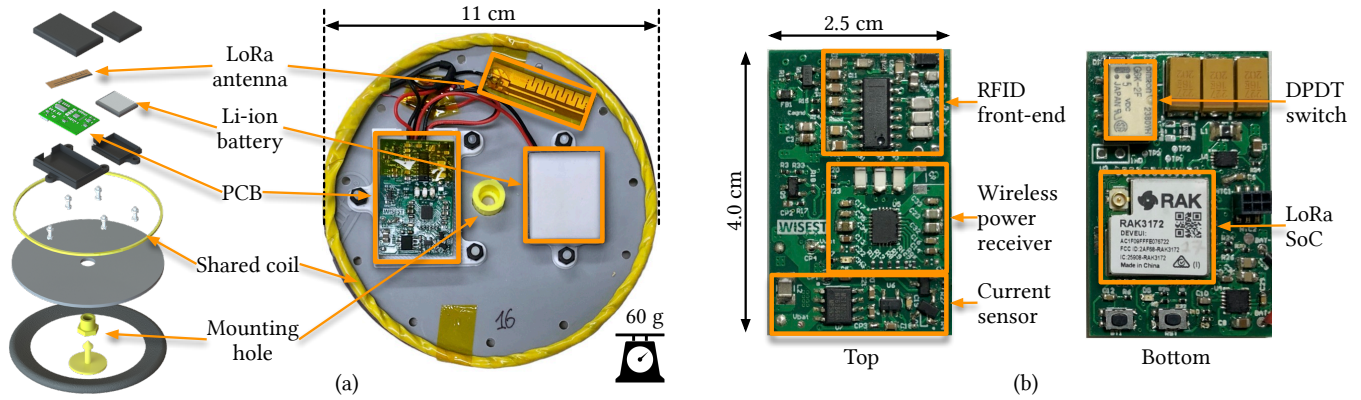


Figure 3: (a) eTAG implementation and assembly before waterproof sealing and (b) detailed view of the PCB (identifying information hidden for anonymity)

Once the optimal coil design is determined, a switching circuit using a double-pole double-throw (DPDT) switch is employed to direct the coil to either resonant circuit to ensure that the scanning and charging circuits operate without interference. By default, the coil is connected to the charging circuit when eTAG is in sleep mode. This ensures that eTAG detects the power transferred from the wireless charger and activates the LoRa SoC when the cow puts her head under the wireless charger. In scanning mode, the switch is controlled to connect the coil to the RFID front-end for scanning the microchip sensor. The duty cycles of microchip sensor scanning and wireless charging are very low; microchip sensor scanning takes less than 1 s and is performed every few minutes, while wireless charging is carried out only for about 10 minutes during milking sessions, once or twice a day. Therefore, eTAG can perform both functionalities using a shared coil with almost no interruption to each other.

4.3 eTAG Implementation

The construction of eTAG is shown in Figure 3(a). eTAG consists of four components: a shared coil, a printed circuit board (PCB), a Li-ion battery, and a LoRa antenna, integrated into an 11-cm circular polypropylene disc.

The shared coil is made of a 32-AWG single-strand magnet wire with 46 turns that provides a good balance between the scanning range, wireless charging performance, and coil temperature increment during charging. As eTAG is to be mounted on top of the ear and may rotate, a round shape is preferred over polygons. This choice ensures uniform scanning performance in all directions and an even distribution of weight on the ear. The inductance of the coil is 650 μ H and the resistance is 11 Ω at 100 kHz; The values of C_{scan} and C_{charge} are 2164 pF and 974 pF, respectively. The resulting resonant frequency of the RFID front-end is 134.2 kHz, which is compliant with ISO 11784/5 [33].

All electronic components including the RFID front-end, wireless power receiver, and power subsystem are integrated

into a small 4.0×2.5 cm PCB as shown in Figure 3(b). The PCB and the battery are protected in 3D-printed plastic cases. To prevent water and dust from entering eTAG and altering the properties of the coil, it is thoroughly sealed with waterproof tape. No noticeable degradation in the scanning range or wireless charging performance was observed after placing other components inside the coil and sealing the device.

To achieve a lightweight design, a small battery is preferred, but a too-small battery would limit the charging current, and will suffer from a more significant voltage drop when the discharge current is high in the scanning mode. A 150-mAh 3.7-V single-cell Li-ion battery is selected to allow a proper charging rate during the short charging session. In comparison to the 45-mAh cell in Section 3.4, a few hundred cycles of the 150-mAh cell are expected for about four years (the typical productive lifespan of a dairy cow). Considering the typical lifespan of Li-ion batteries and the relatively low maximum state-of-discharge (about 30%), the expected battery degradation is minor. We estimate the state-of-charge (SOC) of the battery from its terminal voltage. As the terminal voltage-based battery SOC estimation may be inaccurate if the voltage is measured with a varying current, the impact of varying currents is effectively removed by measuring the terminal voltage only when eTAG wakes up where the discharge current is consistent.

After completely sealed, eTAG is only 60 g, which is light enough to be mounted on the cow’s ear. An even more lightweight implementation could be realized using a commercial-level waterproof casing instead of thick waterproof tape, but we leave this out of the scope of this work.

5 AUTONOMOUS WIRELESS CHARGING OF ETAG

We discuss the wireless power transfer (WTP) technique used for the wireless charger and various design considerations to improve its performance. We also address various problems

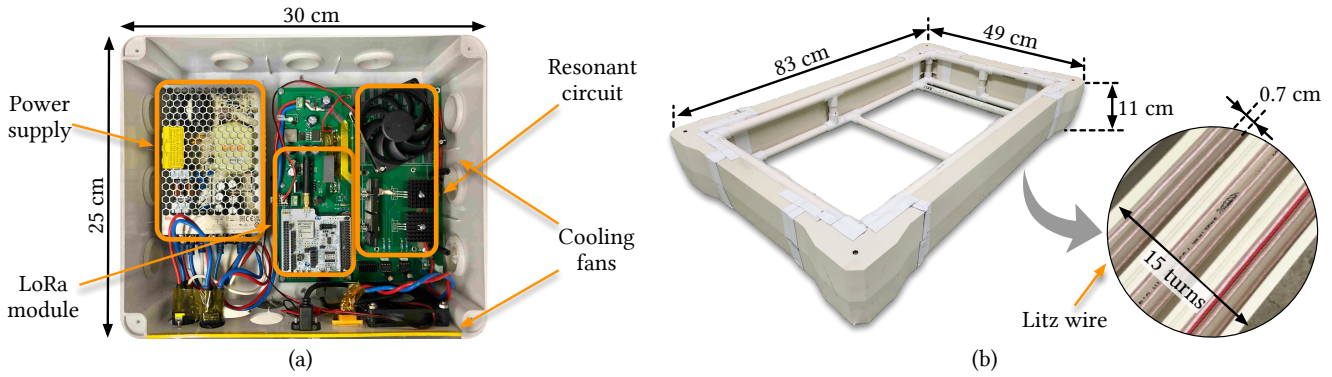


Figure 4: (a) Power supply and controller and (b) primary coil of the wireless charger before waterproof sealing

related to charging eTAG and present a control scheme to ensure high efficiency and safety during charging.

5.1 Optimizing Wireless Power Transfer

The most challenging problem in designing a wireless charger for eTAG is that it is mounted on a moving head. During charging, the position and alignment of eTAG relative to the wireless charger's coil change as the cow moves her head freely, and the distance can significantly vary between 20–70 cm. This results in a variation in the mutual inductance and drastically changes the coupling coefficient. As a result, the amount of power received by eTAG becomes unstable.

In this work, we design the wireless charger to provide a sufficient amount of power to eTAG at an average charging distance of 50 cm (maximum 70 cm). To compensate for the variation in charging power, we design the wireless charger to maximize the charging performance and implement a closed-loop controller to maximize the amount of power that the primary coil emits within a safety limit. First, we adopt various techniques to improve the performance of WPT, such as selecting a suitable circuit topology and refining coil design [54]. The series-series topology is adopted to take advantage of its ability to eliminate power reflection from the load to the power source which helps in increasing WPT efficiency [36]. A high-quality factor coil is implemented using Litz wire. Litz wire contains multiple strands of thin individually insulated wires that help reducing the skin effect at the surface of the wire from AC current, thus reducing energy loss as heat. Also, proper spacing between adjacent turns can increase the maximum quality factor of the coil, as the AC resistance and parasitic capacitance of the coil decrease [16].

An optimal frequency should be selected to safely maximize WPT performance. As the RFID front-end also utilizes resonant inductive coupling to energize the microchip sensor at 134.2 kHz, the wireless charger needs to be designed not to induce current at the microchip sensor while charging. Therefore, 200 kHz is selected for WPT, which is not

a harmonic frequency of 134.2 kHz. Other advantages of the low-frequency WPT are the high adjustment precision for fine-tuning the resonant circuit, and using higher capacitance that allows for the use of capacitor banks where the equivalent resistance can be reduced significantly which reduces losses [53]. In a low-frequency range, the quality factor can be maximized by choosing a proper type of Litz wire [16]. The coil is made of 15 turns of Litz wire (700 strands of 40-AWG wire) with a 0.7 cm gap between adjacent turns, resulting in an effective coil dimension of 83×49×11 cm. Measured at 100 kHz, the inductance of the coil is 290 μ H and the resistance is only 1.8 Ω .

We use a synchronous inverter and a synchronous rectifier to minimize power losses in power conversion at the primary and secondary sides, respectively. Since the received power is used to charge the battery directly, a switch-mode charger is used instead of a linear battery charger to maximize the charging efficiency. In eTAG, as shown in Figure 2, we use an integrated IC as the wireless power receiver that integrates a synchronous rectifier, voltage regulator, and switch-mode battery charger. When the battery is depleted for a long period, this IC can handle charging from cold start with zero energy while the SoC boots up immediately from a very-low voltage to control the charging process.

Figure 4 shows the construction of the wireless charger. Both the electronics box and the coil are sealed for waterproofing, as they are exposed to sprayed water in the milking parlor.

5.2 Charging Performance and Safety

We implement a closed-loop charging controller between eTAG and the wireless charger in order to maximize the charging performance while ensuring the safety of the cows. Considering the short duration of milking sessions, the higher the charging power, the better for energy-neutral operation, but it should not cause any safety risks. As discussed in Section 5.1, the charging power fluctuates depending on the varying position and alignment of the wireless charger and

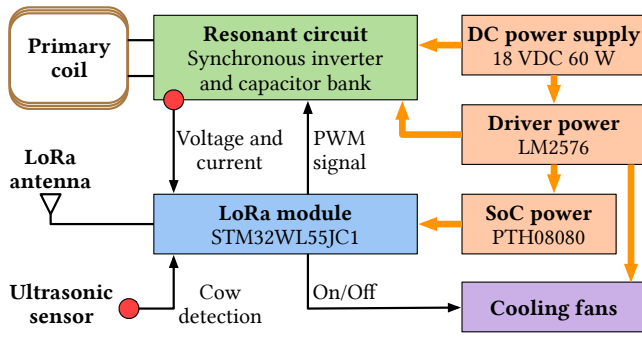


Figure 5: Block diagram of the wireless charger

ETAG due to the movement of the cow’s head. When they are perfectly aligned at a short distance and the level of wireless power is high, ETAG may receive excessive power, which not only heats up the coil but also exceeds the safe charging current threshold of the Li-ion battery. Simply reducing the charging power is not desirable since it will increase the charging time required to achieve energy neutrality. Therefore, our control aims at maximizing the charging power to recharge ETAG as much as possible in a short milking session when it is far from and is misaligned with the charger, while limiting the charging power when the tag is close and well-aligned so that the battery charging current and the coil temperature remain within the safety limits.

The wireless charger communicates with ETAG over LoRa to receive its device status parameters which are required for the closed-loop control. The block diagram of the charger is presented in Figure 5. The primary coil is connected to a resonant circuit consisting of a synchronous inverter and a capacitor bank. When the cow moves into the milking machine with the wireless charger, the charger is automatically activated by an ultrasonic sensor that detects the cow’s presence. The wireless power receiver in ETAG detects the charging power and wakes up its LoRa SoC to enter the charging mode. In charging mode, ETAG periodically measures device status parameters, including the battery voltage, charging current, and coil temperature, and sends them to the charger over LoRa. The LoRa SoC module in the charger, which also controls the charging process, receives the parameters and adjusts the power level at the primary coil. The adaptive controller decreases the charging power if the battery charging current or the coil temperature exceeds their respective thresholds; otherwise, it gradually increases the charging power. The maximum battery charging current is set to 225 mA, which corresponds to 1.5C. The maximum coil temperature is set at 55 °C.

The wireless charger is large enough to cover the range of cow’s head movements. In a tight milking parlor, multiple ETAGs worn by adjacent cows can be under the same charger. When multiple ETAGs are detected, the wireless charger adjusts the charging power in a conservative manner so that

none of the ETAGs violates the safety limits. When there are multiple chargers and multiple tags, each ETAG needs to be paired with only one charger at a time. This can be achieved by chargers advertising their ID through the power channel, where an ETAG that is within the charging range of a charger receives wireless power and extracts the charger ID for charge pairing. Other techniques for exchanging data through the power channel such as NFC does support both slow-rate charging and communication, but it is very short-range, which is not suitable for fast-charging ETAG at up to 70 cm.

Because live animals are involved, the system needs to be safe for the animals and human workers. The maximum allowed level of electromagnetic exposure in humans is defined by the specific absorption rate (SAR) in W/kg. According to two regulatory documents by IEEE [10] and ICNIRP [41], SAR is 2 W/kg for local exposure in unrestricted environments, and a power of 45 W has been shown to be well within this limit [29]. Our design complies with the regulation even when multiple ETAGs are present in the charging area, as the charging algorithm ensures that the charging power never exceeds the safety limit.

6 EXPERIMENTAL RESULTS

We first discuss the experimental setup including microchip sensor injection, ETAG mounting, and wireless charger installation at an operational dairy barn. Measurement results were collected in a three-week experiment from August 15th to September 3rd, 2022, totaling 1966 hours of runtime. Three ETAGs were deployed on three cows in the first week, and four more were deployed on the remaining four cows in the second week. Data was collected at the same time from each individual cow. All sensor deployment procedures (injecting microchip sensors and mounting ETAGs) were done under the approval of the Institutional Animal Care and Use Committee (IACUC) of the University of Wisconsin–Madison (Protocol #A006606). All dairy cattle were handled in compliance to the European Directive 2010/63/EU [43] regarding the protection of animals used for scientific purposes.

6.1 System Deployment

The first task of the deployment of the system is injecting microchip temperature sensors and mounting ETAGs. Each ETAG is mounted in the middle of the ear where there is no blood vessel, while the microchip sensor should be injected into the base closer to a major blood vessel [9]. All the microchip sensor injection procedures are conducted by a licensed veterinarian. Both the microchip and the 12-gauge injection needle are sterilized using an ethylene oxide (ETO) gas autoclave, and the injection site is prepared with 3 mL of lidocaine to minimize any needle injection pain. The distance from the ear base to the middle of the ear is about 7 cm. To achieve the best microchip scanning performance, the

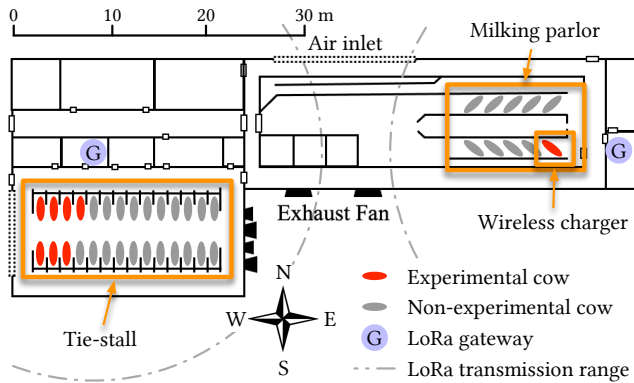


Figure 6: Location of the cows, wireless charger, and LoRa gateways in the dairy barn

microchip sensor is injected in an upward position, at about 2 cm depth into the skin, and is perpendicular to eTAG's coil surface. In a previous study that investigated the effects of microchip sensor insertion in horses [23], it was shown that the sensor did not migrate during six months of the experiment, which indicates the reliability of the injection. Sensor injection did not cause any excessive inflammation or continued tissue irritation in our study. For the verification of the subcutaneous temperature measurement, we use a HOBO Pro V2 temperature logger to record the vaginal temperature of each cow as the reference CBT.

We deployed the system at a dairy facility where 72 Holstein cows are housed. The cows spend most of their time in a tie-stall barn and are milked twice per day at a milking parlor, as shown in Figure 6. To receive and forward LoRa packets from eTAGs effectively, two LoRa gateways were deployed, one at the barn and the other near the wireless charger. The two LoRa gateways cover most of the barn. All packets were sent to an Amazon Web Services (AWS) IoT server in real time.

Figure 7 shows a cow with an eTAG under the primary coil of the wireless charger during milking. The primary coil of the charger is attached to a metal structure, which is a part of the BouMatic Xcalibur 4440 milking system. Mounting the coil to the top frame does not require any modification to the infrastructure nor any special components for the installation. The size and weight of the coil were examined by the barn operator to ensure that it does not affect the cows and the operation of the milking system. We can also see that eTAG mounted on the top of the cow's ear is well aligned with the surface of the wireless charger coil when the cow's head is resting in the milking machine.

6.2 Validation of Temperature Reading

The validity of using subcutaneous temperature at the ear base as a proxy CBT has already been presented in a previous

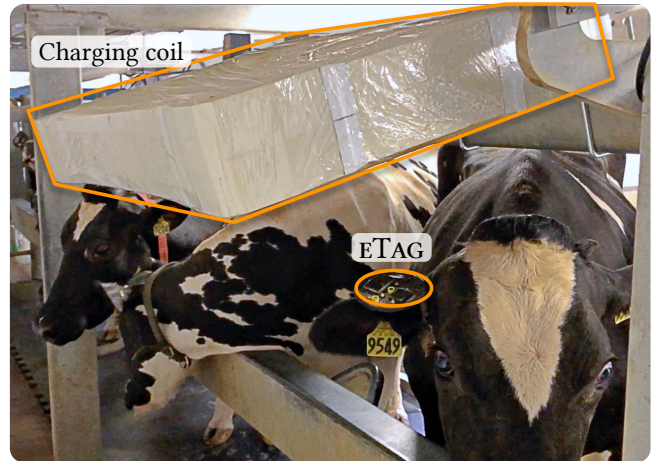


Figure 7: A cow with an eTAG under the wireless charger coil during milking

study [9]. However, we briefly reaffirm this within our system before validating the design of eTAG for energy-neutral sensing of subcutaneous temperature, which is the focus of this study. A sample pattern of subcutaneous temperature measured by eTAG and CBT measured by an intravaginal temperature logger from Cow #7 in a three-day period is shown in Figure 8. Mild weather conditions were recorded during the first half of the period, in which both temperatures were stable within the normal range of rectal temperature for adult Holstein cows from 37.8 to 39.2 °C [13]. However, warm weather conditions (>26 °C and >80% RH) from the second day led to a rise in body temperature by about 1 °C. The ear base temperature showed a comparable data trend as the vaginal temperature, stayed within a 0.5 °C discrepancy with a minimal lag. The vaginal temperature was stable with a smooth trend, while a more fluctuating temperature trend was observed from the ear base. This is likely because cattle's ear is more susceptible to varying external conditions such as ambient temperature, humidity, water spray, and airflow. Nonetheless, these temperature trends indicate a close correlation between the two temperature measurements. The comparison results align with the analysis in [9], further suggesting that ear base temperature can be reliably used as a proxy CBT. This data will help the farmers make timely and informed decisions on cattle management, e.g., relocating cows those are more susceptible to heat stress to better-ventilated areas. It would also enable focused, precision cooling of individual cows using jet cooling fans [31].

6.3 Power Consumption Analysis

Upon every wake-up from sleep mode, eTAG performs several tasks: sensing, scanning, transmission, and reception. During sensing, eTAG measures various device status parameters,

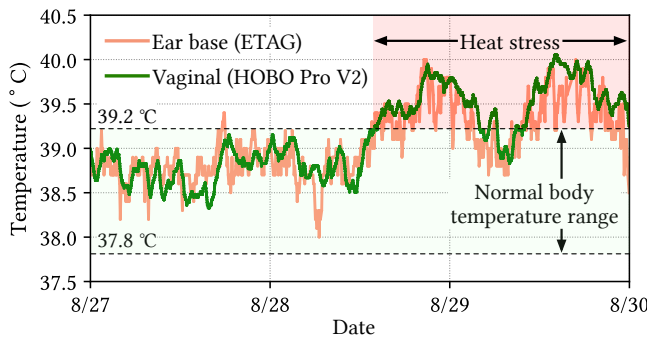


Figure 8: Comparison of ear base temperature measured by eTAG and vaginal temperature from Cow #7 for three days

such as battery voltage, current consumption, and coil temperature. Then, the microchip temperature sensor is scanned by the tag, followed by the transmission task to send the temperature data to the gateway. Subsequently, eTAG switches to the reception task for a short duration to listen for any configuration packet from the gateway before going back to sleep mode for a duration of $T_{wake_intv} = 5$ minutes, during which the total energy consumption is only $E_{sleep} = 45.6$ mJ. This energy consumption mainly comes from the always-on battery management chip for detecting and initiating the charging process.

The duration of the scanning task varies depending on the distance and the orientation of the sensor. The scanning time can be as short as 94 ms when the microchip sensor is close and perfectly aligned with eTAG. If the microchip sensor is not well aligned due to the ear movement, it may take more time to retry to energize the microchip sensor and read data from it. If eTAG does not receive any data from the sensor, the scanning task will timeout after 300 ms to prevent battery depletion. Depending on the success rate of scanning, energy consumption in this task varies from 69 to 219 mJ, resulting in E_{wake} varies from 217 mJ to 367 mJ. As a longer scanning duration results in more energy consumption, better sensor alignment and shorter scanning distance can reduce the scanning time significantly, allowing eTAG to run for a longer duration.

Note that the reception task is only required for reconfiguring eTAG during this test deployment. In commercial usage where reconfiguration is not required, the reception task can be disabled to further reduce power consumption.

6.4 Measurement and Data Collection

The microchip sensor scanning performance and LoRa communication performance of eTAGs are reported in Table 2. Scanning may not always be successful due to the temporary misalignment between eTAG and the microchip sensor, and the success rate varies depending on how the microchip

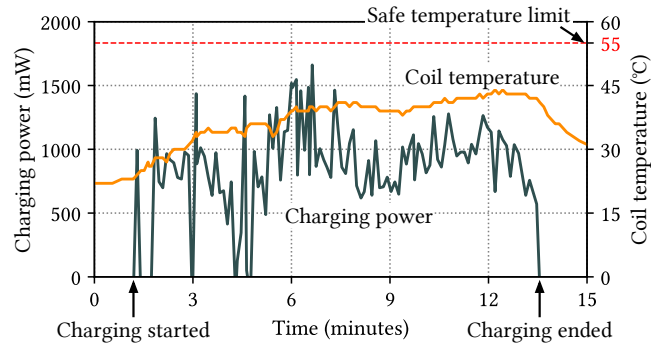


Figure 9: Charging power and coil temperature of Cow #1 during a charging session on August 30, 2022

sensor is injected and how eTAG is mounted. Out of seven eTAGs deployed, six of them exhibited a high successful scanning rate of over 77%; while the other one (Cow #5) was able to successfully scan its microchip sensor 37.7% of the time. This can be attributed to the relatively far location of the mounting hole of Cow #5 from its ear base (as we utilized the existing hole) and the non-ideal orientation of the microchip sensor during injection. However, we believe this can be minimized with more precise injection as experience is gained. Some of the tags were removed due to damage, resulting in shorter durations.

Invalid temperature scanning that falls outside the 35–42 °C range was very rare, with only three cases observed among nearly 20,000 temperature readings. As described in Section 4.1, these results are discarded.

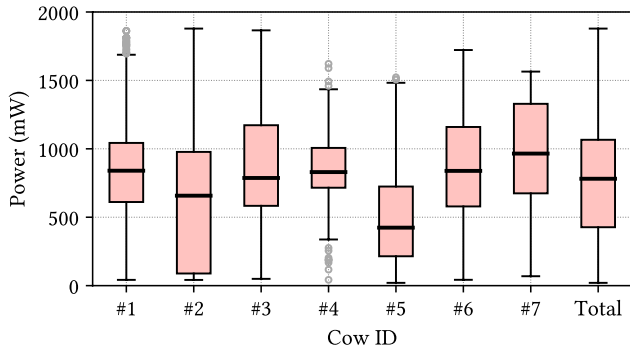
eTAG uses LoRa to report temperature to the AWS server and to transmit the device status parameters to the wireless charger. The reliable communication of LoRa is particularly important for wireless charging control rather than for temperature reporting because the closed-loop control of the charging power relies on the real-time device status parameters. LoRa communication is overall highly reliable, demonstrating success rates of over 99%.

6.5 Charging Performance and Runtime Analysis

Figure 9 shows the charging power and coil temperature variations during a typical charging session. The charging power fluctuated considerably at first when the cow moves into the milking machine. As the cow settles in the position after a few minutes, eTAG starts to align with the wireless charger, leading to stabilized charging power. During charging, the coil temperature of eTAG increases over time, and the wireless charger continuously regulates the amount of charging power to ensure the coil temperature stays safely under 55 °C. The coil temperature regulation was validated in our lab test, but we did not observe any over-temperature

Table 2: Microchip temperature scanning and LoRa communication statistics

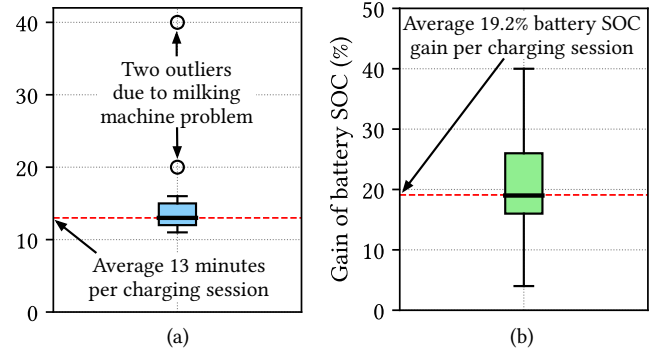
Cow ID	Duration (days)	Number of total scanning	Rate of success scanning (η_{scan})	Number of valid scanning	Number of invalid scanning	Number of received packets	Number of lost packets	Rate of LoRa transmission
#1	19	5905	77.1%	4551	2	7352	44	99.4%
#2	11	3217	94.4%	3038	0	4495	15	99.7%
#3	12	3324	80.0%	2660	1	4076	25	99.4%
#4	5	1345	98.8%	1329	0	1751	5	99.7%
#5	10	2272	37.7%	856	0	2870	6	99.8%
#6	17	4700	89.3%	4197	0	5672	46	99.2%
#7	9	2613	98.0%	2561	0	3012	16	99.5%

**Figure 10: Distribution of varying charging power of 17 charging sessions**

cases during the field experiment where the wireless charger had to reduce charging power.

We conducted a total of 17 charging sessions in the experiment. As shown in Figure 10, the average charging power was around 781 mW. Cow #5 has a relatively poor charging performance because the ear hole was not at the top of her ear, resulting in her eTAG not being well aligned with the wireless charger. The statistical results of the charging duration and the gain of battery SOC after each session are shown in Figure 11. As depicted in Figure 11(a), the charging sessions lasted for about 13 minutes. There were two sessions that lasted for 20 and 40 minutes due to some unexpected technical problems with the milking machine unrelated to our system, causing the cows to stay under the wireless charger longer than usual. Based on these results, a battery with a minimum capacity of 45 mAh at 3.7 V is sufficient for eTAG. Assuming $\eta_{scan} = 79\%$, using (3), eTAG can run for 6.8 days from one charging session. Figure 11(b) shows that the battery SOC increased by almost 20% on average after each charging session when using the 150-mAh cell.

Figure 12 shows the variation of the battery SOC of Cow #3 over eight days. Her eTAG was charged twice during the period, where the two charging sessions are five days apart. The cow was milked twice per day, but she was milked by

**Figure 11: (a) Charging duration and (b) gain of battery SOC of seven eTAG from 17 charging sessions**

other milking machines rather than the one with the wireless charger when charging was not needed. We can see that the final battery SOC of this five-day period (before the second charging) is higher than the initial battery SOC of the period (before the first charging). This indicates that eTAG can perpetually operate with only one charging every five days. Note that the estimated runtime is longer than five days due to the two prolonged charging sessions.

To evaluate how much battery SOC is lost if not recharged, we measure the daily reduction in battery SOC, excluding the days when charging occurred. As shown in Figure 13, about 4% of the battery SOC is consumed every day. As discussed earlier, each charging session recovers battery SOC by about 20%, and thus, eTAG can run for an average of five days on a single charge. Considering the herd size of 72 cows at our testing site, where there are six milking batches per day, based on (6) and the realistic performance of eTAG, only three chargers are required to achieve the energy neutrality of the system.

7 DISCUSSION

Before we conclude our work, we discuss some observations from the deployment and the practical scalability of eTAG.

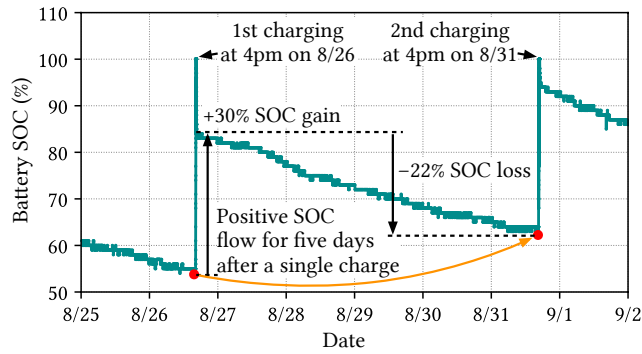


Figure 12: Variation of battery SOC of Cow #3 over eight days with two charging sessions five-days apart

7.1 Cows’ Response to the System

It is important to understand the cows’ behaviors in response to εTAG and the wireless charger before fully deploying the system. As a careful step prior to the experiments described in Section 6.1, we installed the primary coil and mounted an εTAG on one cow for one week before the full deployment. Ear flicking of dairy cattle has been reported to describe the animal’s response to various stressful conditions [18, 25]. We observed the cows before and during the deployment, and noted that the frequency of ear flicks returned to normal after a few days of mounting εTAGs. We also consulted with our animal experts to confirm that there is no significant sign of discomfort. When the cows moved into the milking parlor, some cows showed interest in the wireless charger above their head. They tried to sniff the coil when they first saw it but soon ignored it afterward. The shape and the overhead installation of the coil did not attract their attention nor disturb their routine. Throughout the experiment, we did not observe any significant change in the activity or behaviors of the cows before and after mounting εTAGs.

For a large-scale deployment of the proposed system, a more animal-friendly design of εTAG and wireless charger would be desirable. While we did not observe any noticeable sign of long-term discomfort with εTAG, the biggest challenge is reducing its size and weight, which are largely constrained by the shared coil and the battery. Further optimization of the analog circuitry (RFID front-end and wireless power receiver) and power management can be done.

7.2 Scalability

In practice, the adoptability of the system is largely dependent on the cost of installation. The lab-prototype εTAG, the microchip sensor, and the wireless charger are built from commercially available off-the-shelf components with total costs of USD \$43, \$12, and \$298, respectively. When mass-produced in a commercial setting, the costs would be reduced drastically which would enable a widespread adoption of the system. As modern big dairy barns will increasingly

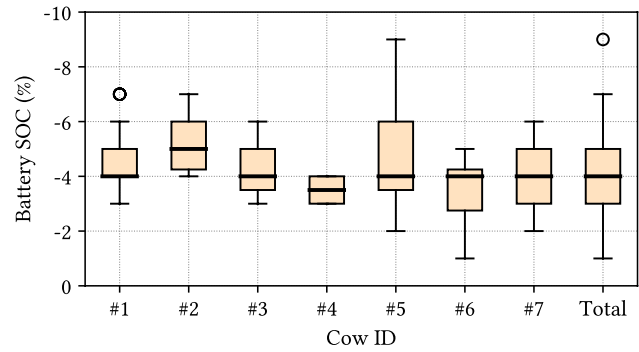


Figure 13: Average daily battery SOC changes of εTAGs during three weeks of deployment

rely more on robotic milking parlors, which can serve multiple cows and identify them through their ID tag, etc., our wireless charger would be easily integrated into these modern milking parlors. εTAG can also include both visual and electronic (RFID) cattle identification that could replace traditional tags entirely. We have consulted with barn operation experts and confirmed that this system is compatible with most modern milking parlors, including access to power.

When scaling up to hundreds of εTAGs, considering the low duty-cycle communication and the density of cows, up to about 100 εTAGs would be manageable per a single-channel gateway [22]. Collision avoidance and ALOHA-like MAC protocols could be used to minimize packet loss when deploying εTAGs on a large scale.

8 CONCLUSIONS

In this work, we introduced a novel system that can collect the body temperature of dairy cows in real time using an autonomously recharged smart ear tag named εTAG to scan an injectable microchip temperature sensor. εTAG is designed to satisfy all critical requirements for a continuous and perpetual body temperature monitoring system for dairy cows. The results from an extensive deployment on seven lactating Holstein cows in a three-week period demonstrate that εTAG can collect and report accurate body temperature of the cows in real time in a minimally invasive way. Our work is the first practical step toward detecting heat stress in a timely manner, which is critical to improving the well-being of dairy cattle as well as the economic, environmental, and social sustainability of the dairy industry worldwide.

ACKNOWLEDGEMENTS

The authors thank the anonymous reviewers for their valuable feedback. This work was supported by the USDA National Institute of Food and Agriculture grant number 2021-67021-34036 and the U.S. National Science Foundation under Grants 1845469, 2112562, and 2213688.

REFERENCES

- [1] Kofi Sarpong Adu-Manu, Nadir Adam, Cristiano Tapparello, Hoda Ayatollahi, and Wendi Heinzelman. 2018. Energy-Harvesting Wireless Sensor Networks (EH-WSNs) a Review. *ACM Transactions on Sensor Networks (TOSN)* 14, 2 (2018), 1–50.
- [2] Ninette K Andersen, Olivier Meyer, Alys Bradley, Nils Dragsted, Anders B Lassen, Ingrid Sjøgren, Julie M Larsen, Warren Harvey, Rastislav Bator, and Aileen Milne. 2017. Evaluation of the PhysioTel™ Digital M11 Cardiovascular Telemetry Implant in Socially Housed Cynomolgus Monkeys up to 16 Weeks after Surgery. *Journal of Pharmacological and Toxicological Methods* 87 (2017), 82–92.
- [3] Ian K. Atkins, Nigel B. Cook, Mario R. Mondaca, and Christopher Y. Choi. 2018. Continuous Respiration Rate Measurement of Heat-Stressed Dairy Cows and Relation to Environment, Body Temperature, and Lying Time. *Transactions of the ASABE* 61, 5 (2018), 1475–1485.
- [4] Said Benaïssa, David Plets, Emmeric Tanghe, Jens Trogh, Luc Martens, Leen Vandaele, Leen Verloock, Frank AM Tuytens, Bart Sonck, and Wout Joseph. 2017. Internet of animals: characterisation of LoRa sub-GHz off-body wireless channel in dairy barns. *Electronics Letters* 53, 18 (2017), 1281–1283.
- [5] Onno Burfeind, Vishal S. Suthar, and Wolfgang Heuwieser. 2012. Effect of Heat Stress on Body Temperature in Healthy Early Postpartum Dairy Cows. *Theriogenology* 78, 9 (2012), 2031–2038.
- [6] Timothy Cavagnaro, Louise Jackson, and Kate Scow. 2006. California Agricultural Landscapes and Climate Change. *Climate Change: Challenges and Solutions for California Agricultural Landscapes* (2006).
- [7] Wen-An Chen, Jih-Tay Hsu, and Ta-Te Lin. 2022. An Automated Thermal Imaging System Based on Deep Learning for Dairy Cow Eye Temperature Measurement. In *2022 ASABE Annual International Meeting*. American Society of Agricultural and Biological Engineers, 1.
- [8] Hanwook Chung, Jingjie Li, Younghyun Kim, and Christopher Y. Choi. 2018. Continuous and Wireless Skin Contact and Ear Implant Temperature Measurements and Relations to the Core Body Temperature of Heat Stressed Dairy Cows. In *10th International Livestock Environment Symposium (ILES X)*. American Society of Agricultural and Biological Engineers, American Society of Agricultural and Biological Engineers, St. Joseph, Michigan, 1.
- [9] Hanwook Chung, Jingjie Li, Younghyun Kim, Jennifer M.C. Van Os, Sabrina H. Brounts, and Christopher Y. Choi. 2020. Using Implantable Biosensors and Wearable Scanners to Monitor Dairy Cattle's Core Body Temperature in Real-Time. *Computers and Electronics in Agriculture* 174 (2020), 105453.
- [10] IEEE Standards Coordinating Committee. 1992. IEEE Standard for Safety Levels With Respect to Human Exposure to Radio Frequency Electromagnetic Fields, 3kHz to 300GHz. *IEEE C95. 1-1991* (1992).
- [11] Grant A. Covic and John T. Boys. 2013. Inductive Power Transfer. *Proc. IEEE* 101, 6 (2013), 1276–1289.
- [12] CubeWorks. 2023. CubiSens™ TS110, Ultra-Small Implantable Wireless Temperature Sensor. Retrieved 2023/07/25 from <https://www.cubeworks.io/product/cubisens-ts110-temperature-sensor/>
- [13] Rodrigo de Andrade Ferrazza, Henry David Mogollón García, Viviana Helena Vallejo Aristizábal, Camilla de Souza Nogueira, Cecília José Verissimo, José Roberto Sartori, Roberto Sartori, and João Carlos Pinheiro Ferreira. 2017. Thermoregulatory Responses of Holstein Cows Exposed to Experimentally Induced Heat Stress. *Journal of Thermal Biology* 66 (2017), 68–80.
- [14] Fabio De Rensis and Rex John Scaramuzzi. 2003. Heat Stress and Seasonal Effects on Reproduction in the Dairy Cow—A Review. *Theriogenology* 60, 6 (2003), 1139–1151.
- [15] Albert De Vries and Marcos I. Marcondes. 2020. Overview of Factors Affecting Productive Lifespan of Dairy Cows. *Animal* 14, S1 (2020), s155–s164.
- [16] Qijun Deng, Jiangtao Liu, Dariusz Czarkowski, Marian K Kazmierczuk, Mariusz Bojarski, Hong Zhou, and Wenshan Hu. 2016. Frequency-Dependent Resistance of Litz-Wire Square Solenoid Coils and Quality Factor Optimization for Wireless Power Transfer. *IEEE Transactions on Industrial Electronics* 63, 5 (2016), 2825–2837.
- [17] Habib Dogan, Ibrahim Bahadır Basyigit, Musa Yavuz, and Selcuk Helhel. 2019. Signal level performance variation of radio frequency identification tags used in cow body. *International Journal of RF and Microwave Computer-Aided Engineering* 29, 7 (2019), e21674.
- [18] PM Faulkner and DM Weary. 2000. Reducing pain after dehorning in dairy calves. *Journal of dairy science* 83, 9 (2000), 2037–2041.
- [19] Fernanda C. Ferreira, Rodrigo S. Gennari, Geoffrey E. Dahl, and Albert De Vries. 2016. Economic Feasibility of Cooling Dry Cows Across the United States. *Journal of Dairy Science* 99, 12 (2016), 9931–9941.
- [20] John W. Fuquay. 1981. Heat Stress As It Affects Animal Production. *Journal of Animal Science* 52, 1 (1981), 164–174.
- [21] Elena Galan, Pol Llonch, Arantxa Villagra, Harel Levit, Severino Pinto, and Agustín Del Prado. 2018. A Systematic Review of Non-Productivity-Related Animal-Based Indicators of Heat Stress Resilience in Dairy Cattle. *PLoS ONE* 13, 11 (2018), e0206520.
- [22] Orestis Georgiou and Usman Raza. 2017. Low power wide area network analysis: Can LoRa scale? *IEEE Wireless Communications Letters* 6, 2 (2017), 162–165.
- [23] Megan I Gerber, Ann M Swinker, W Burton Stanier, Jacob R Werner, Edward A Jdrzejewski, and Ann L Macrina. 2012. Health factors associated with microchip insertion in horses. *Journal of Equine Veterinary Science* 32, 3 (2012), 177–182.
- [24] Alessandro Giro, Alberto Carlos de Campos Bernardi, Waldomiro Barioni Junior, Amanda Prudencio Lemes, Daniela Botta, Narian Romanello, Andréa do Nascimento Barreto, and Alexandre Rossetto Garcia. 2019. Application of microchip and infrared thermography for monitoring body temperature of beef cattle kept on pasture. *Journal of thermal biology* 84 (2019), 121–128.
- [25] Karina Bech Glerup, Pia Haubro Andersen, Lene Munksgaard, and Björn Forkman. 2015. Pain evaluation in dairy cattle. *Applied Animal Behaviour Science* 171 (2015), 25–32.
- [26] Hanns-Christian Gunga, Andreas Werner, Alexander Stahn, Mathias Steinach, Thomas Schlabs, Eberhard Koralewski, Dieter Kunz, Daniel L. Belavý, Dieter Felsenberg, Frank Sattler, and Jochim Koch. 2009. The Double Sensor—A Non-invasive Device to Continuously Monitor Core Temperature in Humans on Earth and in Space. *Respiratory Physiology & Neurobiology* 169 (2009), S63–S68.
- [27] Kevin J. Harvatin and Michael S. Allen. 2005. The Effect of Production Level on Feed Intake, Milk Yield, and Endocrine Responses to Two Fatty Acid Supplements in Lactating Cows. *Journal of Dairy Science* 88, 11 (2005), 4018–4027.
- [28] Gundula Hoffmann, Mariana Schmidt, Christian Ammon, Sandra Rose-Meierhöfer, Onno Burfeind, Wolfgang Heuwieser, and Werner Berg. 2013. Monitoring the body temperature of cows and calves using video recordings from an infrared thermography camera. *Veterinary research communications* 37 (2013), 91–99.
- [29] Shu Yuen Ron Hui, Wenxing Zhong, and Chi Kwan Lee. 2013. A Critical Review of Recent Progress in Mid-Range Wireless Power Transfer. *IEEE Transactions on Power Electronics* 29, 9 (2013), 4500–4511.
- [30] Wataru Iwasaki, Shuichi Ishida, Daisuke Kondo, Yuichi Ito, Jun Tateno, and Michiko Tomioka. 2019. Monitoring of the core body temperature of cows using implantable wireless thermometers. *Computers and Electronics in Agriculture* 163 (2019), 104849.
- [31] Seunghyeon Jung, Hanwook Chung, Mario R Mondaca, Kenneth V Nordlund, and Christopher Y Choi. 2023. Using computational fluid dynamics to develop positive-pressure precision ventilation systems for large-scale dairy houses. *Biosystems Engineering* 227 (2023), 182–194.

- [32] Charles T. Kadzere, Michael R. Murphy, Nissim Silanikove, and Ephraim Maltz. 2002. Heat Stress in Lactating Dairy Cows: A Review. *Livestock Production Science* 77, 1 (2002), 59–91.
- [33] Frans W.H. Kampers, Walter Rossing, and W.J. Eradus. 1999. The ISO Standard for Radiofrequency Identification of Animals. *Computers and Electronics in Agriculture* 24, 1-2 (1999), 27–43.
- [34] Heejin Kim, Younjeong Min, and Byoungju Choi. 2019. Real-Time Temperature Monitoring for the Early Detection of Mastitis in Dairy Cattle: Methods and Case Researches. *Computers and Electronics in Agriculture* 162 (2019), 119–125.
- [35] Andre Kurs, Aristeidis Karalis, Robert Moffatt, John D. Joannopoulos, Peter Fisher, and Marin Soljacic. 2007. Wireless power transfer via strongly coupled magnetic resonances. *Science* 317, 5834 (2007), 83–86.
- [36] Hongchang Li, Jie Li, Kangping Wang, Wenjie Chen, and Xu Yang. 2014. A Maximum Efficiency Point Tracking Control Scheme for Wireless Power Transfer Systems Using Magnetic Resonant Coupling. *IEEE Transactions on Power Electronics* 30, 7 (2014), 3998–4008.
- [37] Jiangjing Liu, Lanqi Li, Xiaoli Chen, Yongqiang Lu, and Dong Wang. 2019. Effects of heat stress on body temperature, milk production, and reproduction in dairy cows: A novel idea for monitoring and evaluation of heat stress—A review. *Asian-Australasian journal of animal sciences* 32, 9 (2019), 1332.
- [38] Sai Ma, Qingping Yao, Takashi Masuda, Shogo Higaki, Koji Yoshioka, Shozo Arai, Seiichi Takamatsu, and Toshihiro Itoh. 2021. Development of noncontact body temperature monitoring and prediction system for livestock cattle. *IEEE Sensors Journal* 21, 7 (2021), 9367–9376.
- [39] Michael Markert, Thomas Trautmann, Florian Krause, Marius Cioaga, Sebastien Mouriot, Miriam Wetzel, and Brian D Guth. 2018. A new telemetry-based system for assessing cardiovascular function in group-housed large animals. Taking the 3Rs to a new level with the evaluation of remote measurement via cloud data transmission. *Journal of Pharmacological and Toxicological Methods* 93 (2018), 90–97.
- [40] S Murugeswari, Kalpana Murugan, S Rajathi, and M Santhana Kumar. 2022. Monitoring body temperature of cattle using an innovative infrared photodiode thermometer. *Computers and Electronics in Agriculture* 198 (2022), 107120.
- [41] International Commission on Non-Ionizing Radiation Protection. 1998. Guidelines for Limiting Exposure to Time-Varying Electric, Magnetic, and Electromagnetic Fields (Up to 300 GHz). *Health Physics* 74, 4 (1998), 494–522.
- [42] Hiroki Ota, Minghan Chao, Yuji Gao, Eric Wu, Li-Chia Tai, Kevin Chen, Yasutomo Matsuoka, Kosuke Iwai, Hossain M Fahad, Wei Gao, et al. 2017. 3D Printed “Earable” Smart Devices for Real-Time Detection of Core Body Temperature. *ACS Sensors* 2, 7 (2017), 990–997.
- [43] European Parliament and Council. 2010. Directive 2010/63/EU of the European Parliament and of the council of 22 September 2010 on the protection of animals used for scientific purposes. *Official Journal of the European Union* 276 (2010), 33–79.
- [44] Liam Polsky and Marina A.G. von Keyserlingk. 2017. Invited Review: Effects of Heat Stress on Dairy Cattle Welfare. *Journal of Dairy Science* 100, 11 (2017), 8645–8657.
- [45] Carolyn L. Stull, Locksley L. McV Messam, Carol A. Collar, Nyles G. Peterson, Alejandro R. Castillo, Buckminster A. Reed, Ken L. Andersen, and William R. VerBoort. 2008. Precipitation and Temperature Effects on Mortality and Lactation Parameters of Dairy Cattle in California. *Journal of Dairy Science* 91, 12 (2008), 4579–4591.
- [46] Vishal Suthar, Onno Burfeind, Britta Maeder, and Wolfgang Heuwieser. 2013. Agreement Between Rectal and Vaginal Temperature Measured With Temperature Loggers in Dairy Cows. *Journal of Dairy Research* 80, 2 (2013), 240–245.
- [47] Philip Thornton, Gerald Nelson, Dianne Mayberry, and Mario Herrero. 2022. Impacts of Heat Stress on Global Cattle Production During the 21st Century: A Modelling Study. *The Lancet Planetary Health* 6, 3 (2022), e192–e201.
- [48] Andrea Vitali, Maria Segnalini, Luigi Bertocchi, Umberto Bernabucci, Alessandro Nardone, and Nicola Lacetera. 2009. Seasonal Pattern of Mortality and Relationships Between Mortality and Temperature-Humidity Index in Dairy Cows. *Journal of Dairy Science* 92, 8 (2009), 3781–3790.
- [49] Joe W. West. 2003. Effects of Heat-Stress on Production in Dairy Cattle. *Journal of Dairy Science* 86, 6 (2003), 2131–2144.
- [50] Jessica B. Wheelock, Robert P. Rhoads, Matthew J. VanBaale, Susan R. Sanders, and Lance H. Baumgard. 2010. Effects of Heat Stress on Energetic Metabolism in Lactating Holstein Cows. *Journal of Dairy Science* 93, 2 (2010), 644–655.
- [51] Jun Yin, Jun Yi, Man Kay Law, Yunxiao Ling, Man Chiu Lee, Kwok Ping Ng, Bo Gao, Howard C Luong, Amine Bermak, Mansun Chan, et al. 2010. A system-on-chip EPC Gen-2 passive UHF RFID tag with embedded temperature sensor. *IEEE Journal of Solid-State Circuits* 45, 11 (2010), 2404–2420.
- [52] Wei Zhang and Chunting Chris Mi. 2015. Compensation Topologies of High-Power Wireless Power Transfer Systems. *IEEE Transactions on Vehicular Technology* 65, 6 (2015), 4768–4778.
- [53] Yiming Zhang, Zhengming Zhao, and Kainan Chen. 2013. Frequency Decrease Analysis of Resonant Wireless Power Transfer. *IEEE Transactions on Power Electronics* 29, 3 (2013), 1058–1063.
- [54] Zhen Zhang, Hongliang Pang, Apostolos Georgiadis, and Carlo Cecati. 2018. Wireless Power Transfer—An Overview. *IEEE Transactions on Industrial Electronics* 66, 2 (2018), 1044–1058.